Manuscript

Whale watching: effects of strong signals on Lippmann style seismometers

Giovanni Romeo

Istituto Nazionale di Geofisica e Vulcanologia

Phone :+39 06 51860305

giovanni.romeo@ingv.it

www.ingv.it

Abstract

In 1982 Erich Lippmann patented a brilliant method to extend the frequency response of seismometers with an electromagnetic transducer. Adopted by Lennartz Electronic this single-coil velocity-feedback strategy appears in a large part of the German company production. In case of strong signals from near events, seismometers using the Lippmann method may produce recordings with a characteristic 'whale-shape'. The article examines the PSPICE (Personal Simulation Program with Integrated Circuit Emphasis) model of an S13 seismometer treated with the Lippmann method, as well as a prototype built in INGV, and shows the effect of strong signals on them.

Keywords:

feedback seismometer

Lippmann method

Single coil feedback

PSPICE simulation

Seismometer saturation

The Lippmann method

A seismometer core is a pendulum, a 2nd order mechanical system.

The goal of a seismometer's designer is to have a nice lightweight broad band instruments (Usher et al, 1978,1979). This is obtained by using some feedback strategy (it is rare, nowadays, to get a good, feedback-free seismometer). In this configuration the mass position is usually detected by means of a displacement transducer and some feedback electronics keeps the mass in place using a current-to-force (voice-coil) actuator (Wielandt and Streckeisen 1982). The observable of interest is picked up somewhere in the feedback loop. The Lippmann (Lippmann and Gebrande 1983) method is different, apparently, because it is a single-coil velocity feedback (Romeo and Braun, 2007). It starts from a geophone, a pendulum with an electromagnetic velocity transducer (1). Here it is possible to induce some damping electromagnetically, by just placing a resistor across the pick-up coil. In this way the damping factor is tied to the geophone parameters by the (2) where G is the pick-up coil gain (tension/velocity), ξ is the damping factor, M the mass, $\omega_0 / 2\pi$ the undamped resonance frequency and R the resistance across the transducer coil.

$$F_{V/vel}(s) = \frac{s^2 a \omega_0^2}{s^2 + 2\xi\omega_0 s + \omega_0^2} \qquad (1)$$

$$\xi = \frac{G^2}{2(R + R_{coil})\omega_0 M} \qquad (2)$$

Fig. 1 shows a geophone response parameterized with the damping factor:
The red track shows a typical geophone velocity response (red track). The blue track corresponds to $\xi = 10$, the green track to $\xi = 50$. A pole (applied to the green track) produces a large velocity flat response (purple track). This is the basic idea. How to increase the damping factor? A dissipative method is not desirable, although possible: we do not want to dissipate the moving mass energy on a passive damper. If we want to do that electrically we need to decrease $R + R_{coil}$ to a value less than R_{coil}, so R must be negative. Negative resistors, obviously are not off-the-shelf parts (Horowitz and Hill, 2006), but may be simulated by a simple electronic circuit that produces, as a useful by-product, some signal amplification.

S13 pSPICE model

The use of a model for simulation is useful, especially to investigate non-linear behavior. Fig. 2 shows a simple S13 (see Geotech manual) model, that uses a Laplace block to simulate the mechanical part. Making some mixed electromechanic simulation requires some perspective change to well understand the observables we have on the schematic. The schematic in Fig. 2 contains indications about the physical meaning in some points.

The model has been checked using a step response (Fig. 3, left) and frequency response (Fig. 3, right).

The Lippmann electronics.

Fig. 4 shows a simplified schematic to implement the Lippmann method on the S13. The first op amp is used to simulate a -3300 Ohm resistor. The damping resistor applied to the ideal (0 Ohm) pick up coil becomes 300 Ohm, so inducing a damping factor $\xi = 25$ and obtaining, after the pole introduced by U2, a segment of flat velocity response. Fig. 5 shows the behavior of Fig. 4 model, excited with a step of 50 mA on the calibration coil (left) and with a velocity sweep (1mm ground displacement) on the right.

Electronics saturation

In case of strong local events, the Lippmann enhanced seismometers show whale-shaped recordings like the ones in Fig. 6. This, of course, is not a natural signal, but is produced by the physical implementation of the Lippmann method. The zero line of the seismogram becomes a curve and an apparently good seismogram follows this wrong reference. We say 'apparently good' because we do not observe any clipping or distortion of the waveform when it is plotted relative to the wavy zero line. Before we believe that we obtained a good seismogram we must remember that the method introduces a low frequency pole on the signal path: this is a low-pass which can mask the effect of clipping with its strong smoothing effect. Therefore, if we are looking for saturation, we need to investigate the negative resistor stage (u3 in Fig. 4). The current on the simulated negative resistor flows trough the real resistor R12. U3 reaches saturation conditions when its output voltage (current on the damping resistor multiplied by R12 value) exceeds the power supply voltage.

An approximate estimate is given by the transfer function that ties the coil current to the ground velocity.

$$\frac{I(s)}{V(s)} = \frac{Ms^2G\frac{1}{R}F(s)}{1+sG^2\frac{1}{R}F(s)} \qquad (3)$$

Equation (3) can be inferred from the model in Fig. 2. *I(s)* is the coil current, *V(s)* the ground velocity, R the damping (coil resistance + negative resistance) resistor. In the worst case (R→0) (3) may be written as:

$$I(s) = sMV(s)\frac{1}{G} \qquad (4)$$

Or, in the time domain, for a sinusoidal velocity excitation $V_0 \sin(\omega \cdot t)$,

$$i(t) = \frac{V_0 \omega M}{G}\cos(\omega t)$$

$$V_0 \cdot f < \frac{G \cdot V_{sat}}{2\pi M \cdot (R_{12} + R_{coil})} \qquad (5)$$

Where G is the motor coil gain (Volt/(m/s)), M the oscillating mass (Kg), R12 is the resistor used in the negative impedance converter, R_{coil} is the pick-up coil resistance and V_{sat} is the U3 saturation voltage (Fig. 4).

Inequality (5) approximately establishes a threshold in the frequency*amplitude product for a Lippmann seismometer: above this threshold the seismometer malfunctions.

Model saturation

The seismometer's behavior in case of strong signals may be understood using the PSPICE model. To do this we employed a normalized impulsive velocity stimulus (6), derived from a Gaussian ground (Fig. 7) displacement, using values above and below the threshold established by equation (5).

$$P(f,t,t_0) = 6f\sqrt{e}(t-t_0)e^{-18f^2(t-t_o)^2} \qquad (6)$$

Equation (6) produces a simple, normalized, frequency tunable, excitation. Of course this is not a continuous harmonic stimulus, but it is easier to study the model comportment with this simple stimulus than using a continuous wave.

Giving a 1Hz and 0.007 m/s speed stimulus (below the threshold $V_0 \cdot f = 0.01$ m/s) the seismometer is not saturated. Fig. 8 shows (A) the forces acting on the mass, the one induced by the acceleration (blue), and the one induced by the feed-back (red). They are very similar, and the mass movement is very weak (B). The seismometer's output is shown in C. It is not exactly a copy of the excitation, but this in accord with the transfer function. Fig. 9 shows, like Fig. 8, the seismometer's behavior; this time the excitation (1Hz at 0.009 mm/s) very close to the $V_0 \cdot f = 0.01$ threshold gives appreciable saturation effects, without saturating the output stage. Fig. 9(A) shows the forces acting on the seismometer's oscillating mass: in this case the force induced by the ground acceleration is not compensated by the feedback force: the electronics just cannot supply such force, and the track appears distorted. This results in an excessive mass displacement B that keeps a finite value even after the stimulus ends. This happens because the mass displacement at the and of the stimulus, given by (neglecting the spring force)

$$displacement = \frac{1}{M} \iint_{stimulus\_length} (Feed\_force(t) - Acc\_force(t))dt^2$$

is different from 0 if the feedback force is different from the stimulus force. At the end of the stimulus the mass displacement has a finite value that the spring tries to compensate. This requires a long time, tens of seconds in the model examined, and, in this time the pole block integrates the signal, producing the characteristic whale-shaped output D . The D diagram shows two tracks, labelled 'DC coupled' and 'AC coupled'. The dc coupled is the one produced by the model shown. The 'ac coupled' is produced introducing a pole-zero couple in the output circuit (i.e. a RC high-pass filter). This is a useful engineer's trick to kill some unwanted dc bias that may be produced by too many dc-coupled amplifiers. This trick causes, as a result, the output to go below 0V, producing the "whale" tail, absent in the dc-coupled track.

Whale's shape

As just shown, a whale-shape is the product of the decay of the overdamped oscillator filtered by the pole and by the 'ac-coupling' zero-pole pair.

A very over-damped oscillator ($\xi >> 1$) decaying waveform is described, by

$$x(t) = e^{\frac{-t\omega_0}{2\xi}} \qquad \dot{x}(t) = \frac{-\omega_0}{2\xi} e^{\frac{-t\omega_0}{2\xi}} \tag{8}$$

Or, in the Laplace space: $$X(s) = \frac{-\omega_0}{2\xi\left(s + \frac{\omega_0}{2\xi}\right)}$$

Equation (8) describes the waveform we expect from the negative resistor output after saturation. The complete whale-shape that we expect may be written, in the Laplace space:

$$W(s) = \frac{-\omega_0}{2\xi\left(s + \frac{\omega_0}{2\xi}\right)} \cdot \frac{a}{s+a} \cdot \frac{sb}{sb+1} \tag{9}$$

where $\frac{a}{s+a}$ is the Lippmann method pole (Fig. 1), and $\frac{sb}{sb+1}$ represents the anti-offset ac coupling. In the time domain (inverse Laplace transform of (9)) the whale-shape may be written as:

$$w(t) = 2abc\xi\left[\frac{-\omega_0}{(2a\xi-\omega_0)(2\xi-\omega_0 b)}e^{\frac{-t\omega_0}{2\xi}} - \frac{a}{(2a\xi-\omega_0)(ab-1)}e^{-at} + \frac{1}{(ab-1)(2\xi-\omega_0 b)}e^{\frac{-t}{b}}\right] \tag{10}$$

where c is an amplitude coefficient. Consequently, fitting a measured whale-shape with the (10), may determine some characteristic of your seismometer. Unfortunately, since the whale-shape is unpredictably triggered by a non linear behaviour, cleaning the seismogram by subtracting the whale-shape may not work for the first part of the seismic event, when the "whale" has been triggered.

Simulating a real event

The model has been tested using the signal from the 2009 L'Aquila earthquake. The signal from the mainshock, recorded by a Kinemetrics Episensor FBA-3 (NS component) 23 km far from the epicentre (Fig. 10) has been used, changing the amplitude to study the effect on the simulated sensor. The amplitude of the signal has been changed using a scale factor x (x=0.1,0.2..0.4) to evidence the effect of the amplitude on the whale-shape signal occurrence. The mass displacement is a nice indicator to identify the non-linear response, Fig. 11 shows the mass displacement obtained with different amplitude signals. The negative resistor damper tries to restrict the mass position variation (it tries to stop the mass velocity) and it is successful until scale factor is 0.3. When the signal exceeds threshold equation (5) (scale factor 0.4) the damper force is not strong enough, and the mass position increases dramatically. The spring force tries to restore the mass position, but this happens slowly because of the damper (8).

How does this affect the seismometer's output? Fig. 12 shows three seismograms, obtained, like in Fig. 11, feeding the seismometer's model with signals with three scale factors, 0.2, 0.3 and 0.4. The output has been normalized by dividing by the same scale factor used for feeding (just a cosmetic effect). The effect of this operation on an ideal linear device should be nothing: three identical tracks. But, because of the negative resistor op-amp saturation the 0.4 scaled track shows a whale-shape.

How dangerous can a "whale" be? A small "whale" cause few trouble. Fig. 13 shows the 0.2 scaled and the 0.4 scaled recordings. The 0.4 scaled track was filtered to remove the whale-shape. The seismograms appear very similar even in the most critical zone (between 35 and 45 seconds, Fig. 12). So it seems we may safely remove a weak whale-shape without affecting the seismogram. Although Fig. 13 encourages using seismograms just subtracting "whales", the whale-shape presence indicates some instrument saturation, and there is no guarantee about the safe use of a cleaned seismogram.

Whale signal polarity

During a strong excitation the mass displacement (Fig. 11) shows unpredictable values, determined by the shape of the stimulus and by the maximum current the negative resistor op-amp can supply.

When the stimulus ends, the mass keeps the position last assumed; the seismometer spring, damped by the negative resistor tries to restore the equilibrium position. Therefore the sign of this force (the sign of the "whale") depends of the last position the mass had just before the end of the saturation condition.

Fig. 14 represents the effect of several sinus bursts on a Lippmann seismometer. The frequency of the bursts was 1.5 Hz and the amplitude was enough to saturate the negative resistor op amp but not the output integrator. The bursts length spans from 3 to 4 seconds, in steps of 0.05s. The span extent has been chosen to be a little greater than the signal period. Fig. 14 (left) shows the seismometer's output, where "whales" are randomly spread. Of course this does not happen descending below the negative resistor saturation threshold (Fig. 14, right)

Conclusion.

A pSPICE model of a Lippmann seismometer has been examined to determine the origin of the whale-shape that, in case of strong signals, appears superimposed over an apparently correct signal. The origin of this malfunctioning has been identified as originated by the saturation of the negative impedance converter used in this kind of seismometers. A closed math form has been written to describe the whale-shape.

Acknowledgements

I thank Thomas Braun who gave me the idea to write down this note and installed and operated some S13 Lippmann-enhanced stations. I thank Paolo Benedetti, who built the electronics. I thank Francesco Mele and Alfonso Mandiello who supplied the data used in simulations. A special thank to Stephen Monna for enlightening suggestions and encouragements.

References

Geotech instruments LLC. PORTABLE SHORT-PERIOD SEISMOMETER MODEL S-13 – Operation and maintenance manual. http://www.geoinstr.com/pub/manuals/s-13.pdf. Accessed 13 April 2011

Horowitz , P., Hill, W. (2006) The art of electronics. Cambridge University Press, Lippmann,E.,H Gebrande (1983).Eine einfache Methode zur Erweiterung des Meβereichs elektrodynamischer Seismometer. Annual meeting of the German Geophysical Society, Aachen.

Romeo, G. abd Braun, T. (2007) . Appunti di sismometria. Quaderni di Geofisica 46. http://portale.ingv.it/portale_ingv/produzione-scientifica/quaderni-di-geofisica/archivio/quaderni-di-geofisica-2007. Accessed 13 April 2011

Usher, M.J., C. Guralp and R. F. Burch (1978): The design of miniature wideband seismometers *Geophys. J. R. Astr. Soc*. 55, 605-613

Usher, M.J., R.F. Burch and C. Guralp (1979): Wide-band feedback seismometers. Physics of earth and planetary interiors 18, pp. 38-50.

Wielandt, E. and G. Streckeisen (1982): The leaf-spring seismometer: design and performance. *Bull. Seis. Soc. Am.*, vol. 72, No 6, pp. 2349-2367.

Zahradník J., Pleŝinger A., (2010) Toward Understanding Subtle Instrumentation Effects Associated with Weak Seismic Events in the Near Field. Bulletin of the Seismological Society of America; February 2010; v. 100; no. 1; p. 59-73

Captions

Fig. 1 How the Lippmann method works. An overdamped (green track) geophone (red track) is lowpassed (purple track) with a pole below the geophone corner frequency, so extending the velocity low frequency response.

Fig. 2 The S13 pSPICE model, designed using the Laplace block to schematize the seismometer's mechanical part. It has two inputs, ground speed (1 volt at the input is equivalent to 1 m/s) and current through the calibration coil, and one output, the voltage on the pick-up coil. Pick-up coil inductance and capacity don't appear in the model because their effect is negligible in the frequency range used in simulation.

Fig. 3 On the left the model behavior when excited with a step (a 1g weight placed on the oscillating mass or 50 mA on the calibration coil). On the right the velocity response with a 1 m/s sinusoidal excitation.

Fig. 4 The two op amps circuit applies the Lippmann method to the S13 geophone. U3 simulates a negative resistor of -3300 Ohm. The op amp U2 adds a 0.1s pole to the transfer function.

Fig. 5 Step response (50 mA through the calibration coil) and frequency response (1mm ground displacement) of fig 4 model. Comparing the S13 response in fig3 and the Lippmann-upgraded response may give the idea about the value of this method.

Fig. 6 A whale-shaped recording obtained using a 20 s Lennartz seismometer (green trace) and a 50s Lippmann enhanced S13 (purple trace). Arezzo, Italy, seismometer on the epicentre, M = 3.2, 7 km deep.

Fig. 7 The velocity stimulus to feed the simulated seismometer has been produced using the derivative of a bump displacement. The variable *f* determines the centre frequency, t_o the position in the time axes. This derivable continuous function has a null integral, so it is a nice stimulus for the model and does not induce undesirable offsets.

Fig. 8 A simulated ground bump displacement (according to fig 7). A shows that the restoring force and the ground movement force are in perfect agreement, the real mass displacement is negligible B, and the seismometer's output agrees with the excitation into the transfer function limit C.

Fig. 9 A simulated ground bump displacement (according to fig 7). A shows that the restoring force and the ground movement force are not in agreement: the restoring force appears distorted and when the stimulus disappears, has a finite value. The real mass displacement is higher than expected, and keeps a not negligible value when the stimulus disappears B. The first part of the seismometer's output apparently agrees with the excitation C , but, at the end of the stimulus, a whale-shaped wave is produced D.

Fig. 10 The 2009 L'Aquila mainshock acceleration has been used to stimulate the seismometer's model.

Fig. 11 The effect of different amplitudes on the mass displacement. When the signal amplitude is less than the threshold (equation(5)), the displacement is of just few microns, otherwise it grows quickly.

Fig. 12 The effect of changing amplitude on the seismometer's output. The instrument operates correctly until the scale factor 0.4, when the "whale" occurs.

Fig. 13 The seismogram with scale 0.4 after "whale" removal, and the uncorrupted seismogram (scale 0.2) appear identical, even in the most critical part (between 35 and 45 seconds) when the "whale" is triggered.

Fig. 14 Left: a Lippmann seismometer output, fed with variable length bursts able to saturate the negative resistor op-amp. Since the saturation condition point moves with the length of burst, “whales” are spread out. Right: the same seismometer fed with bursts insufficient to saturate the negative resistor op-amp.

colour figure

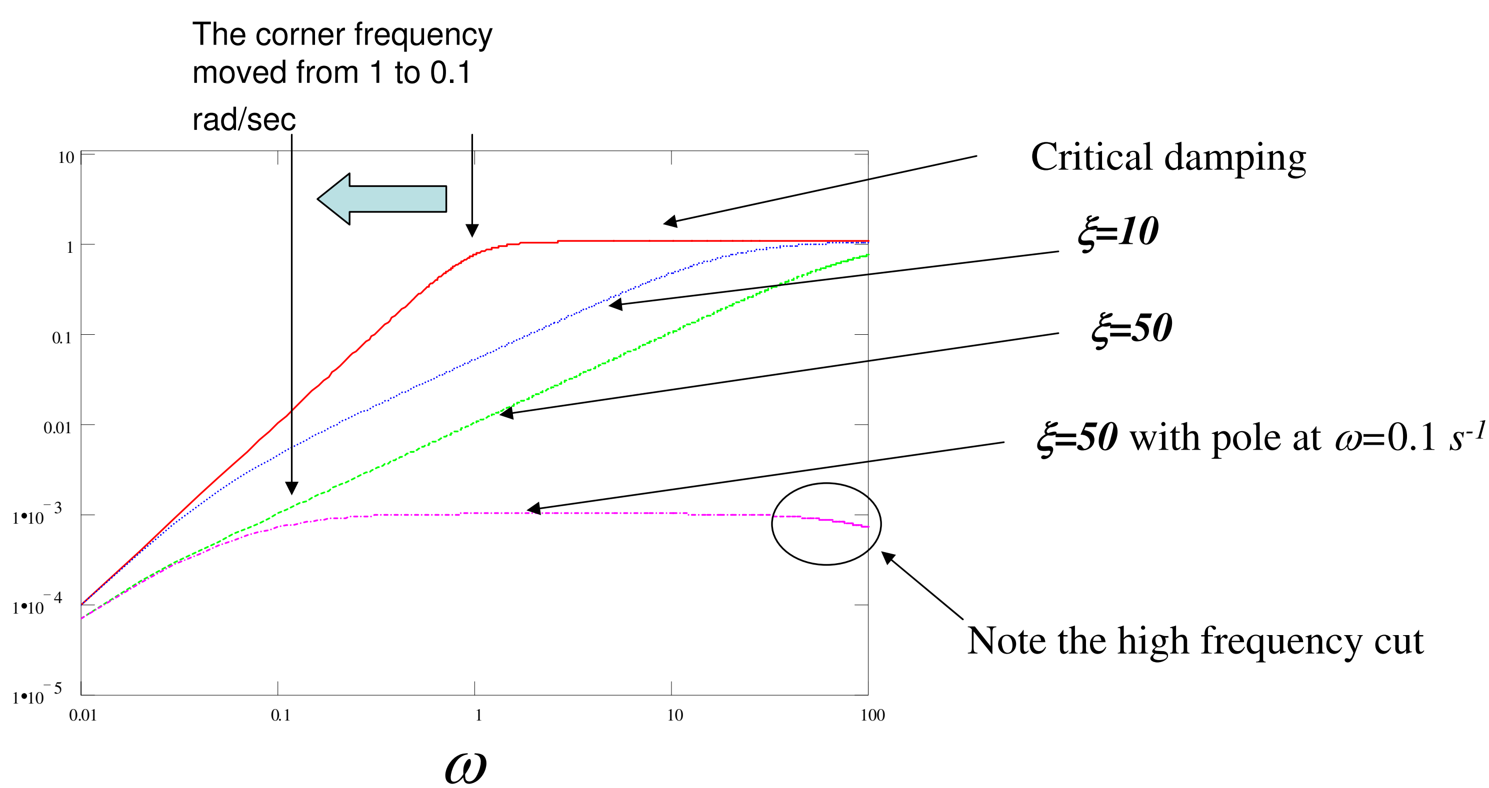

colour figure

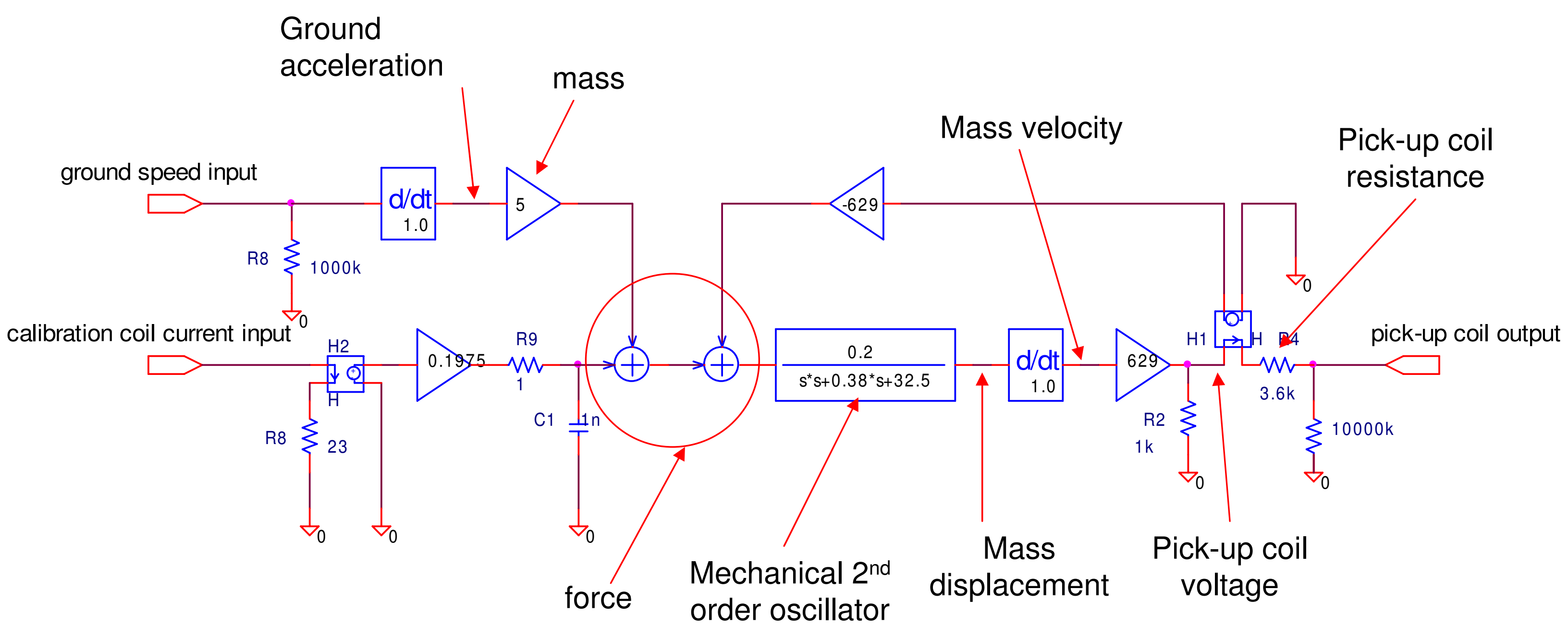

colour figure

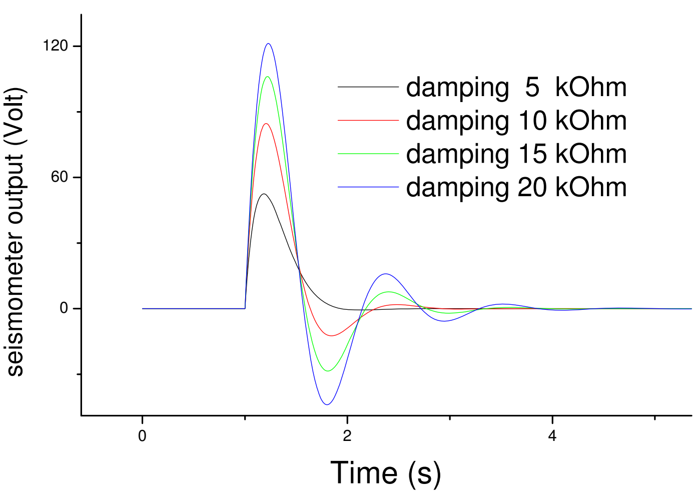

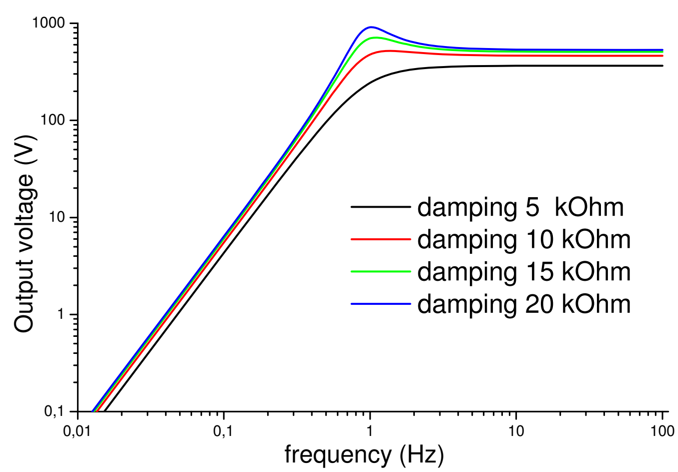

colour figure

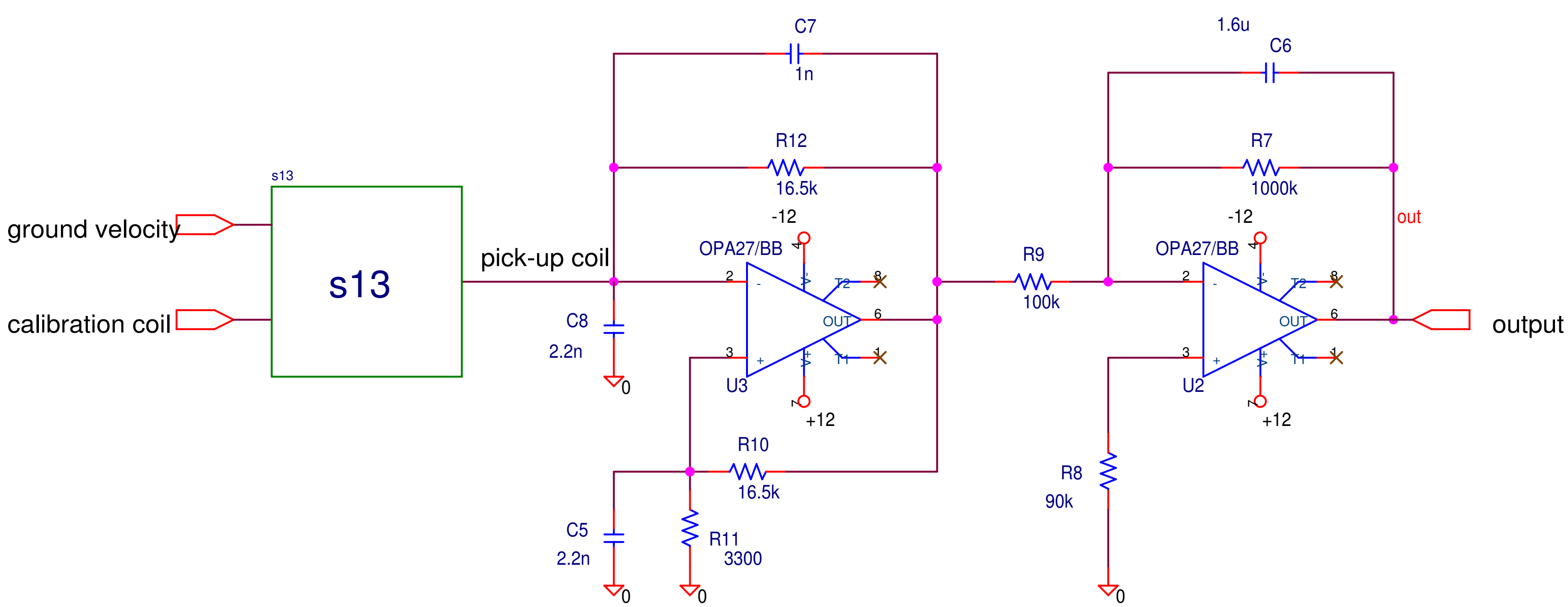

colour figure

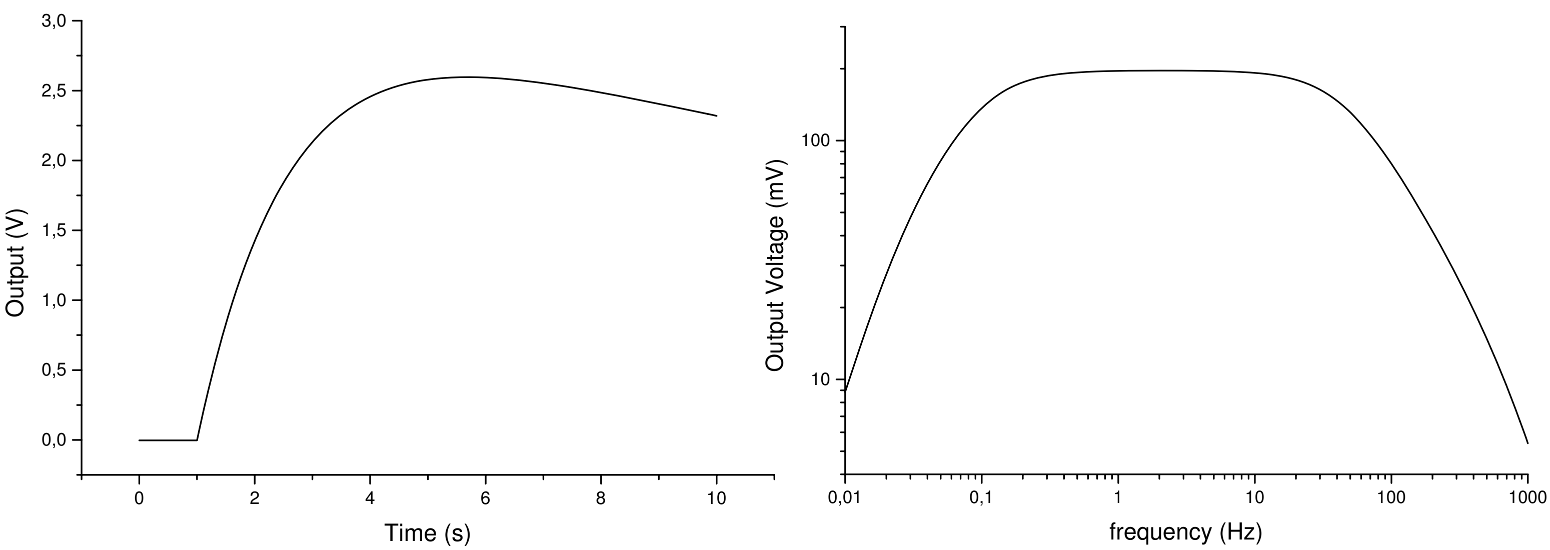

colour figure

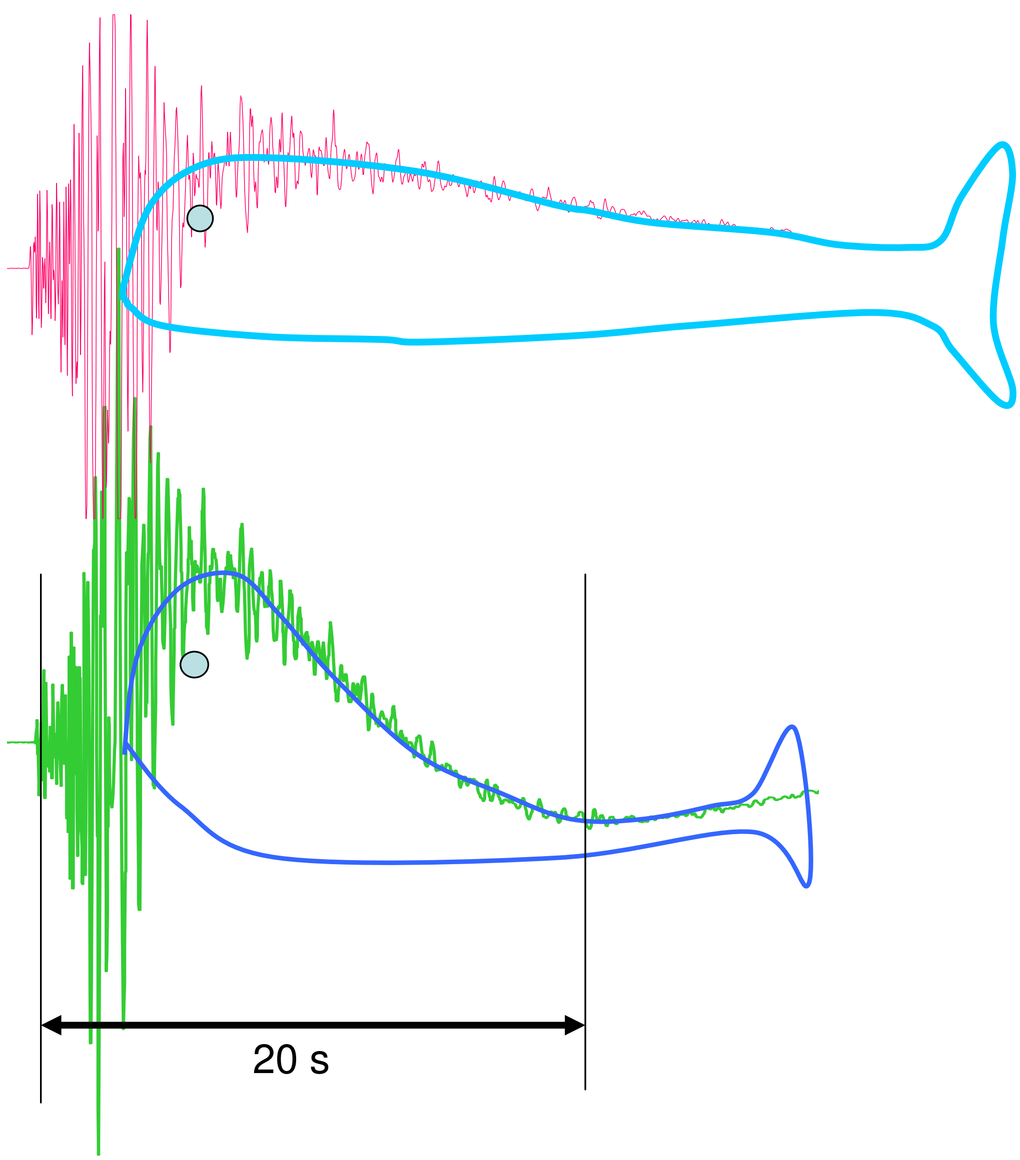

colour figure

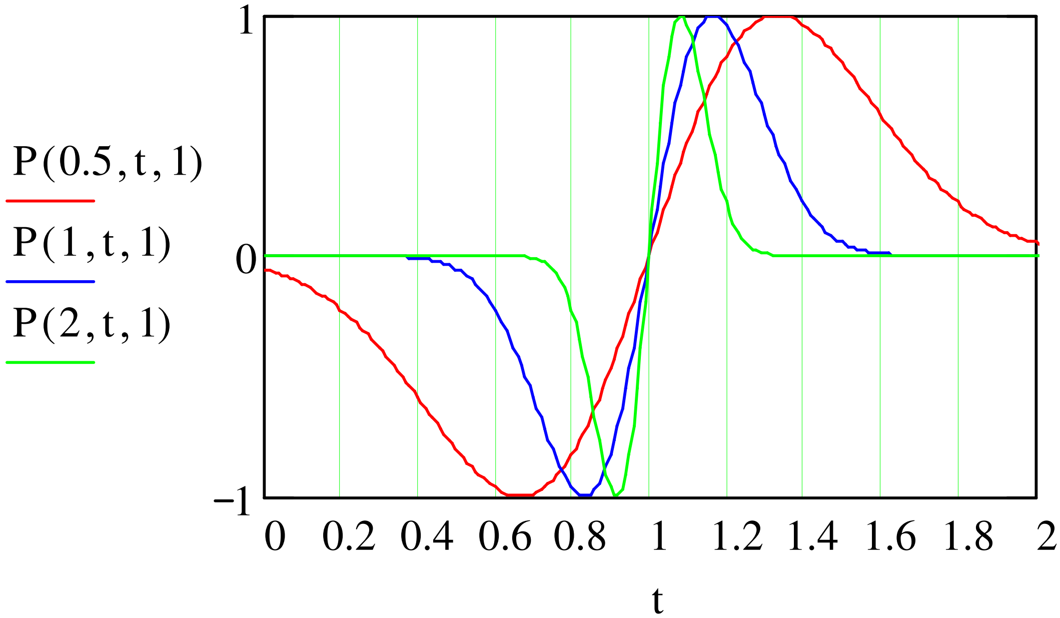

colour figure

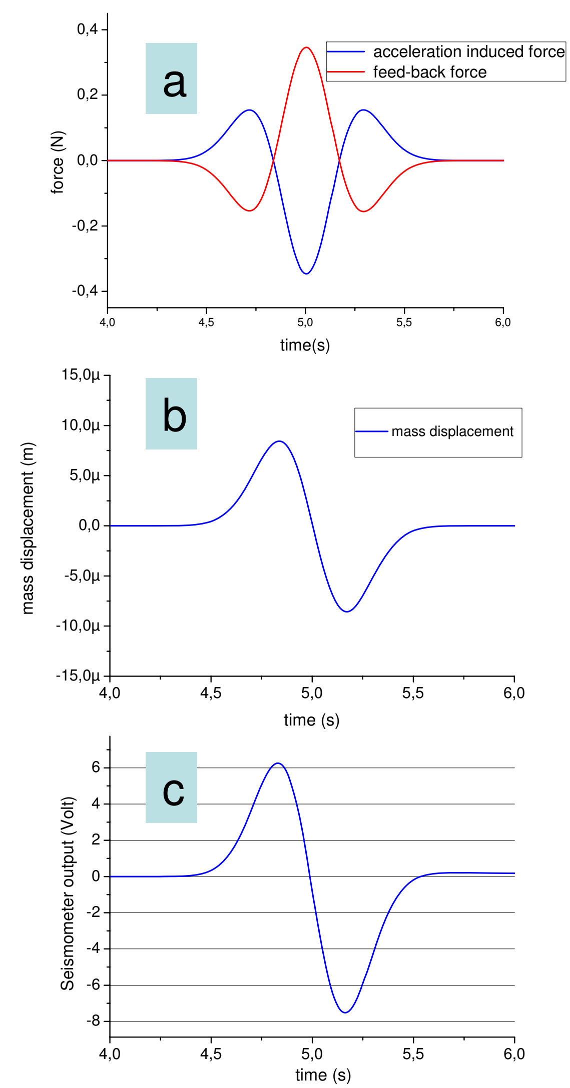

colour figure

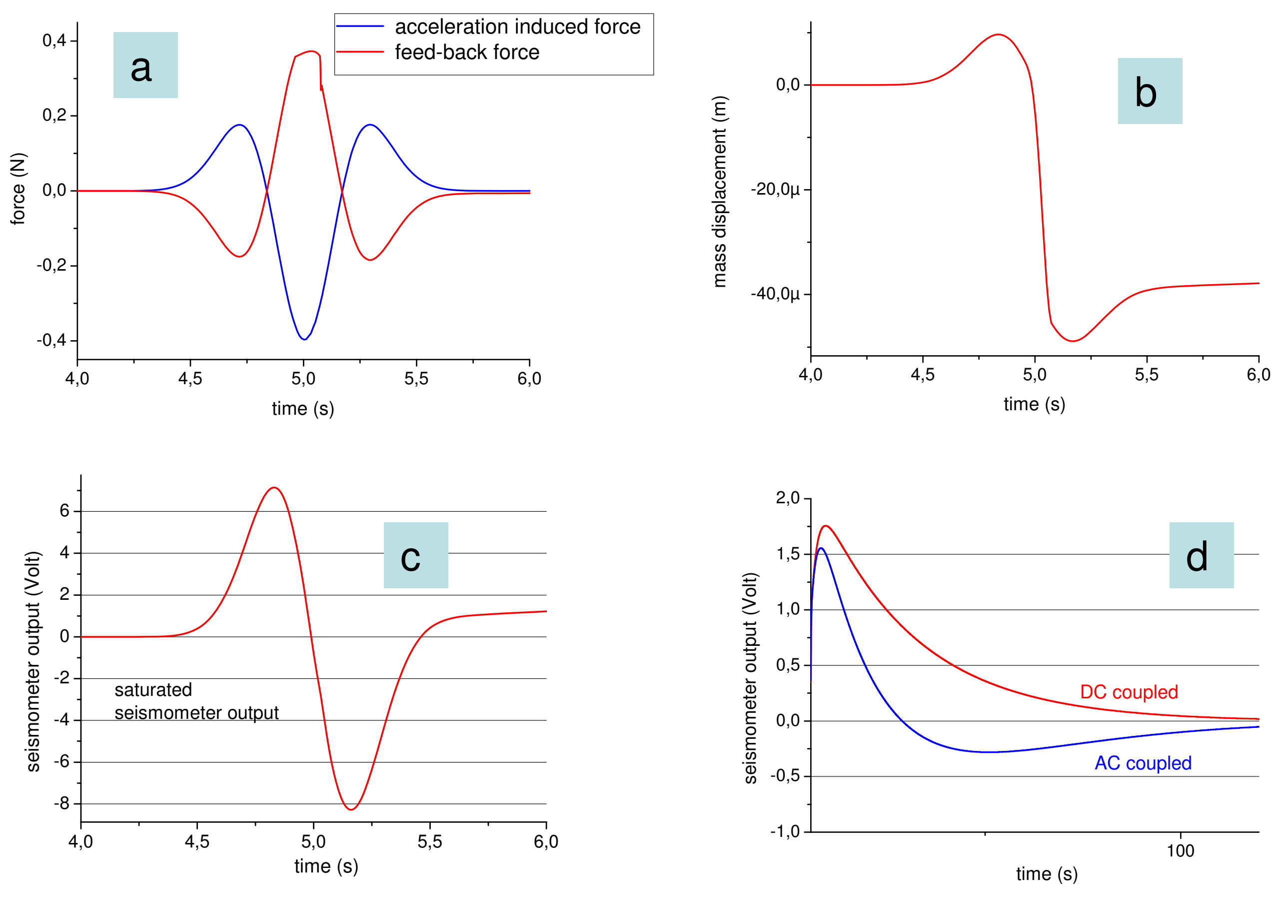

colour figure

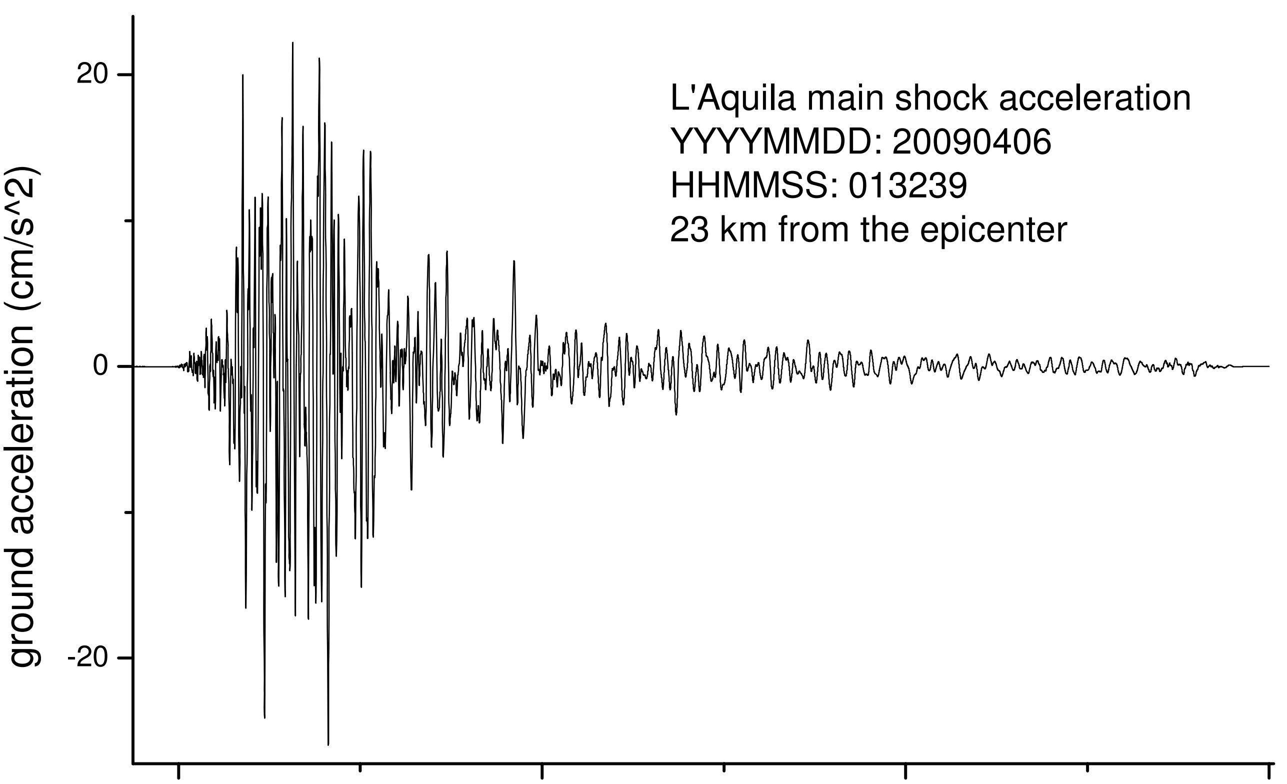

colour figure

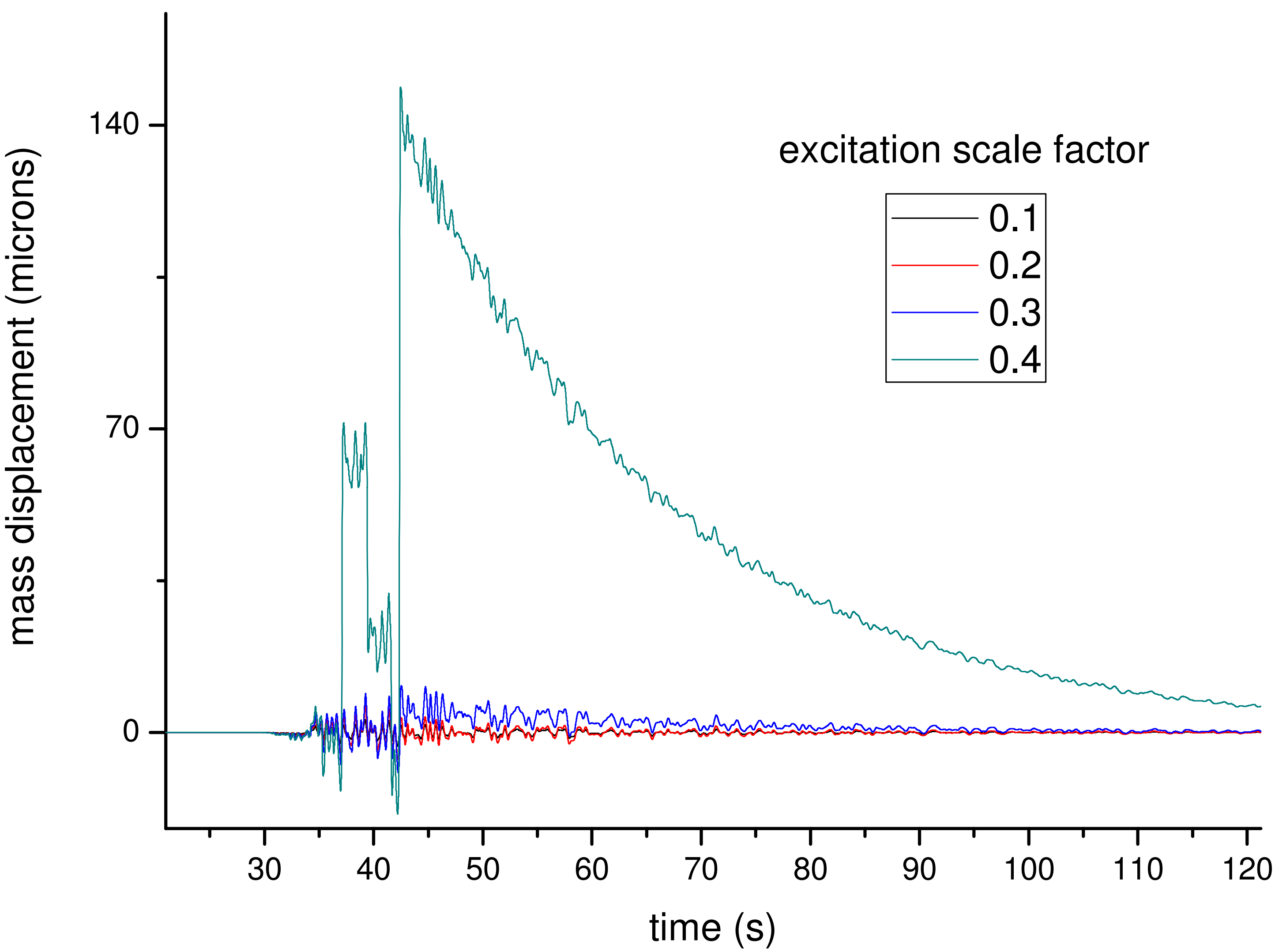

colour figure

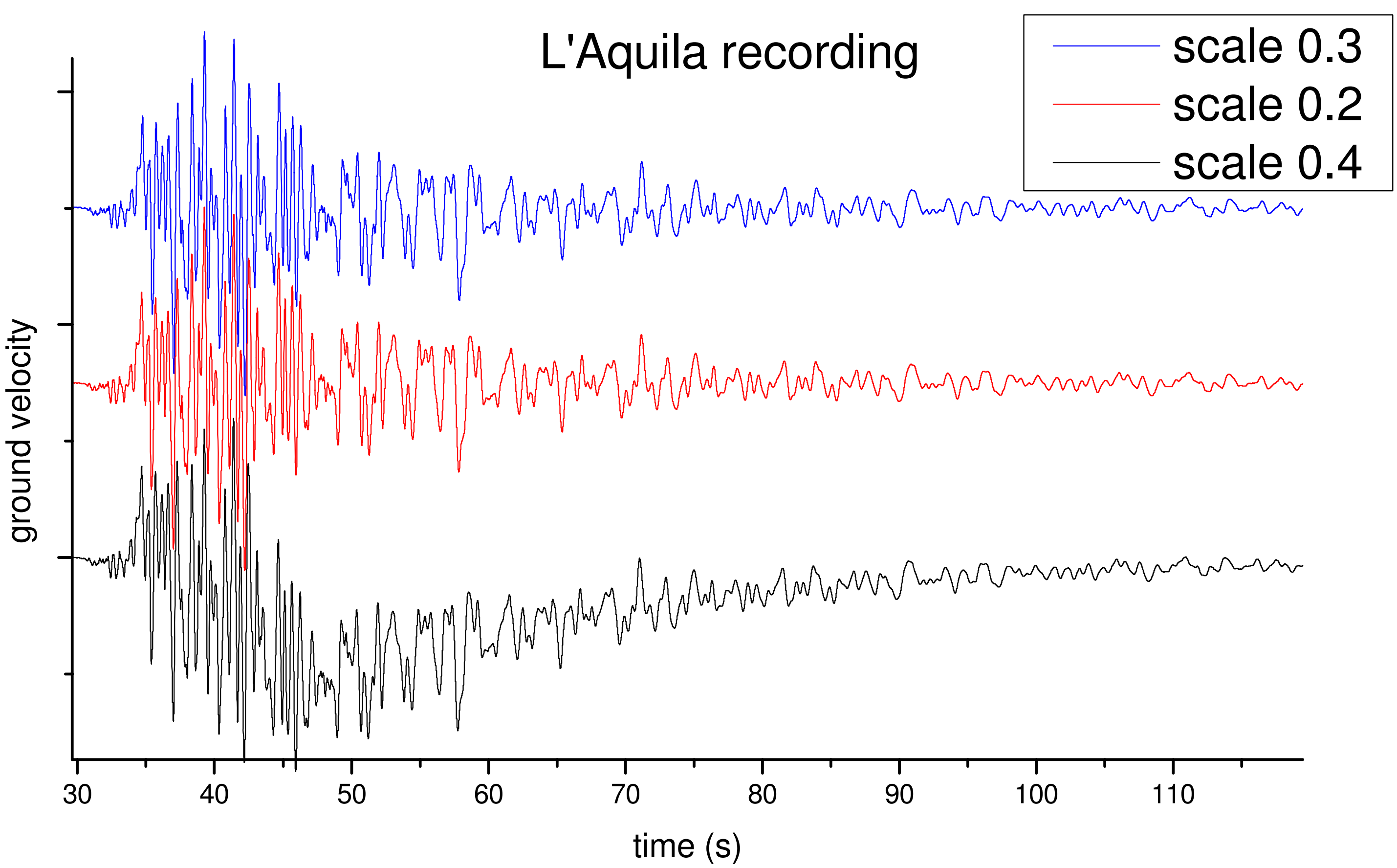

colour figure

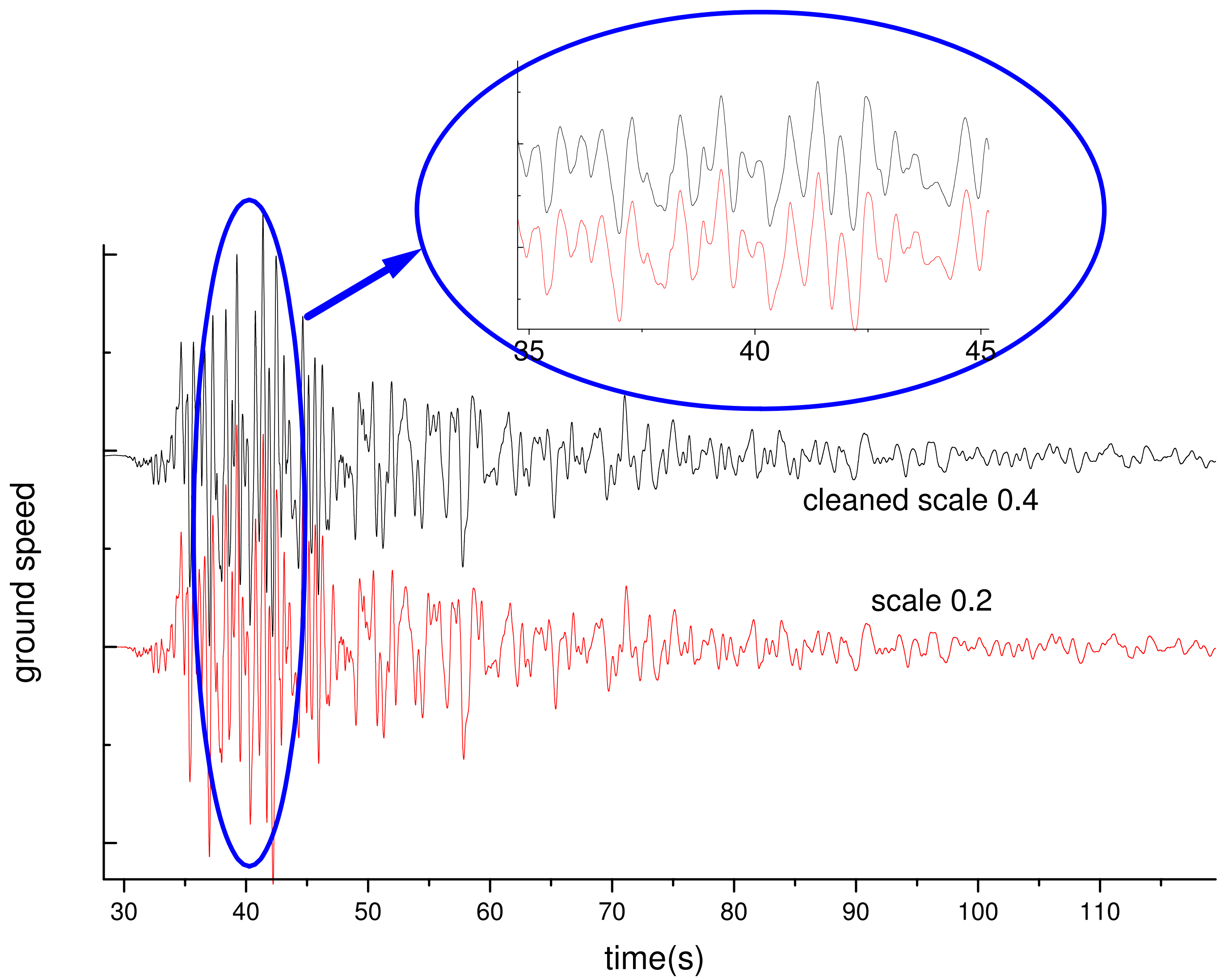

colour figure